Bacteria Sensing

DOI: 10.1002/anie.200703369

# Rapid and Efficient Identification of Bacteria Using Gold-Nanoparticle–Poly(*para*-phenyleneethynylene) Constructs**

*Ronnie L. Phillips, Oscar R. Miranda, Chang-Cheng You, Vincent M. Rotello,* and Uwe H. F. Bunz**

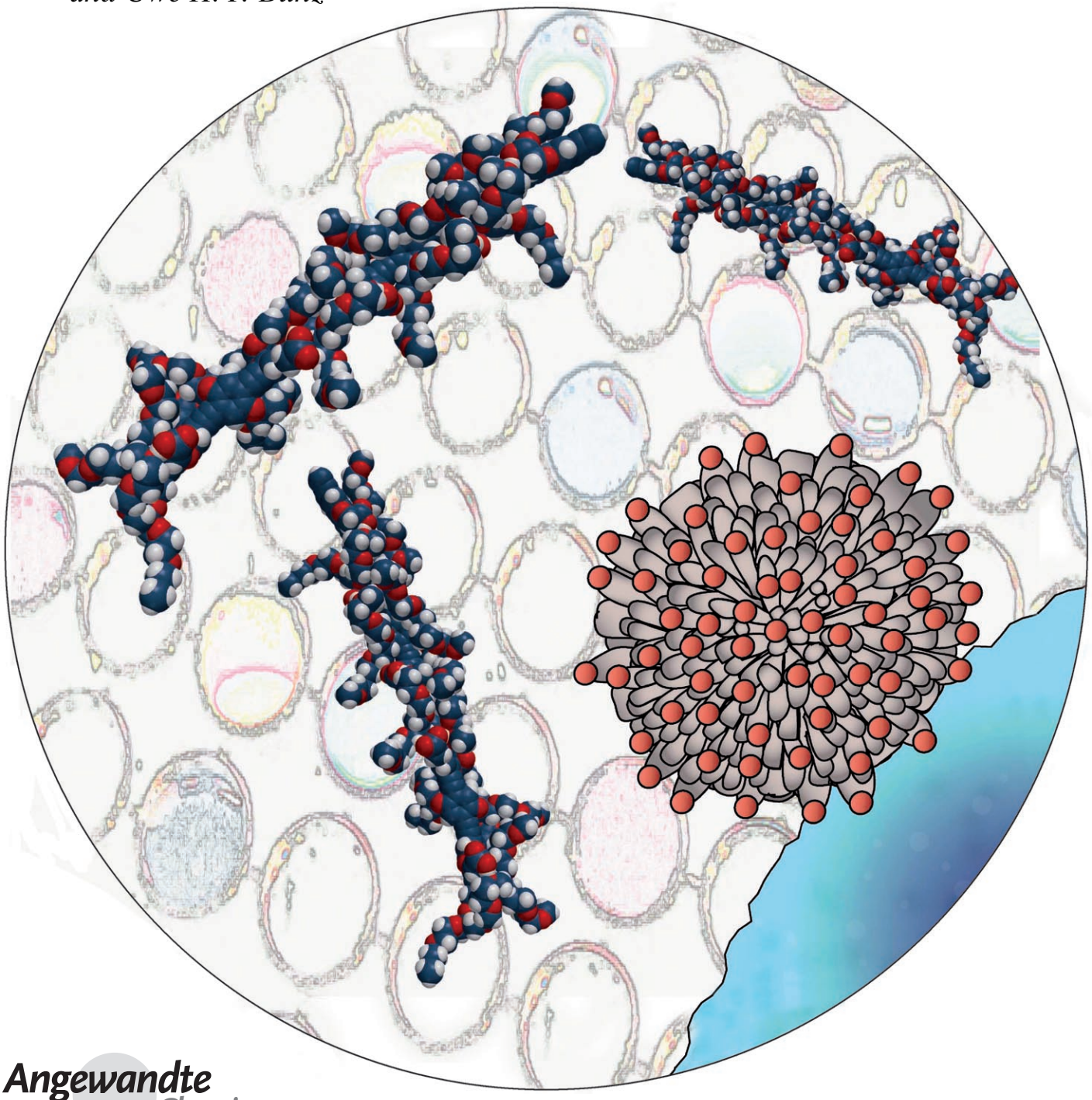

Fast and efficient identification of pathogens in water and biological fluids is an important issue in medical, forensic, and environmental sciences.[1,2] We demonstrate herein that noncovalent conjugates of gold nanoparticles and poly(*para*-phenyleneethynylene) (PPE) identify bacteria effectively within minutes.[3–8] Nanoparticle–bacteria interactions release the bound fluorescent polymer from the gold-nanoparticle quencher, turning on of the polymer fluorescence. The differential fluorescence responses generated by the bacterial surfaces provide an efficient means of identification.[5] We have tested the efficacy of this method by using twelve different bacteria, demonstrating our ability to differentiate between species of bacteria as well as between strains of a single species, without the use of antibodies[6,7] or radioactive markers.[8]

Conventional plating and culturing[9] is generally used to identify causative bacterial pathogens in clinical environments. Although technologically advanced systems have been developed for specific microorganisms,[10] these methods are complex or require sophisticated instrumentation. Plating and culturing is accurate, but requires significant time and effort (more than 24 h). Point-of-care treatment decisions are therefore made without access to microbiological information, potentially leading to the prescription of a suboptimal antibiotic. An example is the treatment of keflex- or methicillin-resistant *S. aureus* strains (MRSA) in community-acquired infections that require treatment with either sulfa drugs or vancomycin.[11] Reisner and Woods have investigated over 9000 cases of clinically reported bacterial infections,[9] and found that 85–90% were due to only seven pathogens, with *S. aureus* and *E. coli* being responsible for half of all infections. A simple and rapid test that could discern the clinically most prevalent pathogens would be of great value, providing effective therapeutics against causative pathogens to be administered during the initial point-of-care visit in over 85% of all cases. This capability would not only increase the efficacy of therapy, but would also reduce the occurrence of drug-resistant bacteria arising from inappropriate use of antibiotics.

The detection of bacteria and pathogens likewise plays a crucial role in food safety.[12] For example, *E. coli* O157:H7 is a world-wide cause of foodborne illness, and is responsible for more than 2000 hospitalizations and 60 deaths directly related to bacterial infection each year in the United States.[7,13] Major outbreaks were associated with the contamination of unpasteurized juice, vegetables, water, etc.[14] However, testing food for contamination is difficult owing to the complex and/or lengthy analysis protocols.

To address the issue of rapid identification of bacteria, a procedure has been developed for bacterial sensing using an array of gold-nanoparticle–conjugated polymer constructs.[15,16] This sensing procedure adopts the concept of the "chemical nose", where a series of analyte receptors are combined to differentiate targets according to their unique response diagrams. As shown in Figure 1, an anionic PPE is initially associated with cationic gold nanoparticles in aqueous solution to afford fluorescence-quenched complexes. In the presence of bacteria, the surface of which is always

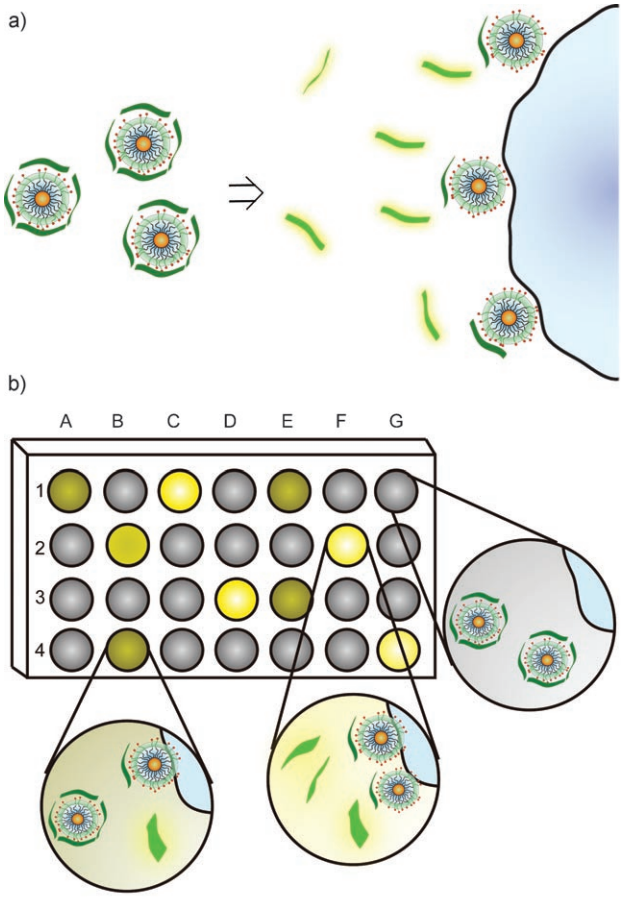


***Figure 1.*** Design of the nanoparticle–conjugated polymer sensor array. a) Schematic representation of the displacement of anionic conjugated polymers from cationic nanoparticles by negatively charged bacterial surfaces. b) Schematic illustration of fluorescence pattern generation on a microplate. In case of release from the nanoparticle, the initially quenched PPEs regain their fluorescence. The fluorescence response is dependent upon the level of displacement determined by the relative nanoparticle–PPE binding strength and bacteria–nanoparticle interactions. By modulating such interactions, the sensor array may generate distinct response patterns against different bacteria. In the diagram, A–G on the microplate represent bacteria of different types, and codes 1–4 represent the PPE–nanoparticle constructs.

[*] R. L. Phillips, Prof. Dr. U. H. F. Bunz
School of Chemistry and Biochemistry, Georgia Institute of Technology
901 Atlantic Drive, Atlanta, GA 30332 (USA)
Fax: (+1) 404-385-1795
E-mail: uwe.bunz@chemistry.gatech.edu

O. R. Miranda, Dr. C.-C. You, Prof. Dr. V. M. Rotello
Department of Chemistry, University of Massachusetts
710 North Pleasant Street, Amherst, MA 01003 (USA)
Fax: (+1) 413-545-2058
E-mail: rotello@chem.umass.edu

[**] This work is supported by the Department of Energy (DE-FG02-04ER46141, U.H.F.B and V.R.) We thank Dr. A. Bommarius (Georgia Institute of Technology) and Dr. J. Hardy (University of Massachusetts Amherst) for donation of the bacterial stocks.

Supporting information for this article is available on the WWW under http://www.angewandte.org or from the author.

  

negatively-charged, the anionic PPE is released. Thus, after the addition of bacteria to the nanoparticle–PPE conjugate, fluorescence is restored as a consequence of the presence of free PPE.[16] Polylysine-functionalized gold nanoparticles with a diameter of 1.6 nm[17] recognize patches of hydrophobic/functional surfaces on microorganisms, and poly(L-lysine)-coated gold nanoparticles self-assemble with live bacteria through complementary electrostatic interactions.[18–21]

The π-conjugated polymer used in this study provides both multivalency[19] and the molecular wire effect[20] to facilitate efficient signal generation in the sensing process. As functional patches (that is, the charged residues and hydrophobic "hot spots") are prevalent on cell and microbial exteriors,[21] this strategy has potential applications in the identification of a wide variety of microorganisms.

For the fluorophore displacement strategy, we chose **Sw-$CO_2$**[22] and three hydrophobic ammonium-functionalized gold nanoparticles (**NP1**–**NP3**)[16] as sensor elements (Figure 2). Fluorescence titration studies revealed that the

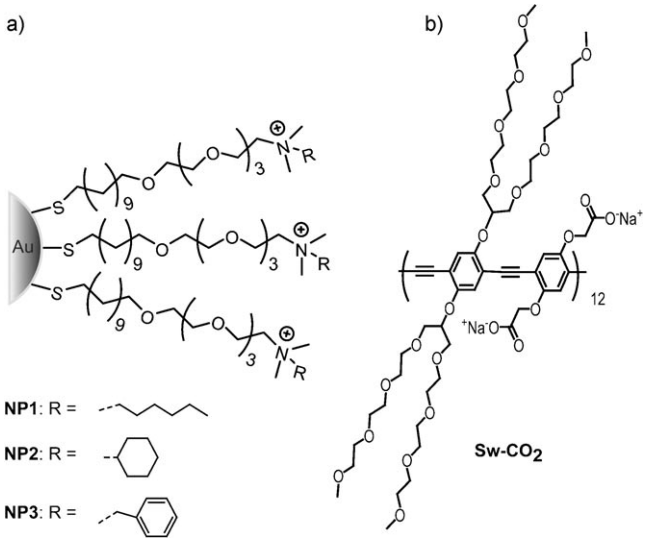


***Figure 2.*** Receptor and transducer components of the bacterial sensors. a) Structural representation of three cationic gold nanoparticles (**NP1**–**NP3**) with various hydrophobic tails. b) Chemical structure of the conjugated polymer (**Sw-$CO_2$**) featuring a branched oligo(ethylene glycol) side chain to suppress non-specific polymer–microorganism interactions.

cationic gold nanoparticles (**NP1**–**NP3**) quench the fluorescence of **Sw-$CO_2$** by formation of supramolecular complexes (see Figure S1 and Table S1 in the Supporting Information).[15] Quenching by the nanoparticle is efficient: typically, an aqueous solution of the polymer (100 nM, based on twelve repeat units per polymer) is titrated with a stoichiometric amount of nanoparticle until the fluorescence drops to approximately 20% of the initial fluorescence of **Sw-$CO_2$** ($\Phi = 0.33$). The polymer and a stoichiometric amount of nanoparticles (**NP1**–**NP3**) were mixed in 5 mM phosphate buffer (pH 7.4) to yield nanoparticle–**Sw-$CO_2$** constructs with final polymer and nanoparticle concentrations of 100 nM and 10–40 nM, respectively. The exposure of these three nanoparticle–**Sw-$CO_2$** constructs to bacteria ($OD_{600} = 0.05$) induced different levels of fluorescence changes (Figure 3). In most cases, the fluorescence of the solution increases upon

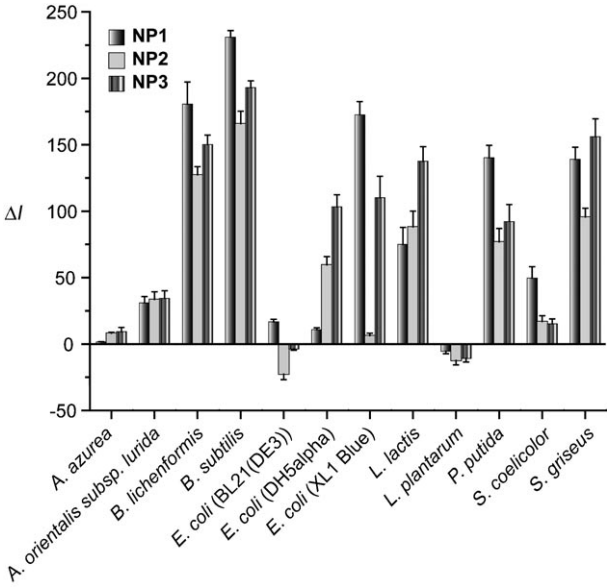


***Figure 3.*** Fluorescence response patterns of nanoparticle-polymer constructs in the presence of various bacteria ($OD_{600} = 0.05$). Each value is an average of six parallel measurements, and the error bars are shown.

addition of the microorganisms. Significantly, the fluorescence changes are reproducible, and depend upon the strains and classes of bacteria, indicating differentiation in the fluorophore displacement. The twelve different bacteria display excellent separation when the fluorescence changes were plotted in a three-dimensional graph with the fluorescence change of the three nanoparticles (**NP1**-**NP3**) as the respective axes (Supporting Information, Figure S1), explicitly demonstrating the ability of these particles to discriminate between bacteria.

In selecting nanoparticles that would constitute the sensor array, both hydrophilic and hydrophobic nanoparticles were tested. Upon incubation with bacteria, however, only the hydrophobic ones (**NP1**–**NP3**) produced significant fluorescence recovery. As hydrophobic and hydrophilic nanoparticles exhibit comparable binding affinities to **Sw-$CO_2$**, the significant difference in the fluorescence recovery indicates that the former strongly interact with bacteria. A plausible explanation is that the hydrophobic parts of the nanoparticles interact with hydrophobic regions on the surface of the bacteria (e.g., the alkyl chains in teichoic acid), enhancing the electrostatic nanoparticle–bacteria interaction and, thereby, the fluorescence regeneration. Therefore, both electrostatic and hydrophobic interactions seem to play important roles in the complexation of these particles with bacteria. We plan to engineer nanoparticles with varying size, shape, and hydrophobicity to augment the diversity in the fluorescence response patterns.

  

The fluorescence response patterns were analyzed by linear discriminant analysis (LDA), a quantitative statistical method extensively used in pattern recognition.[23–24] Discriminant functions were deduced by maximizing the separation between classes relative to the variation within classes; LDA (Figure 4) transformed the raw patterns to canonical scores

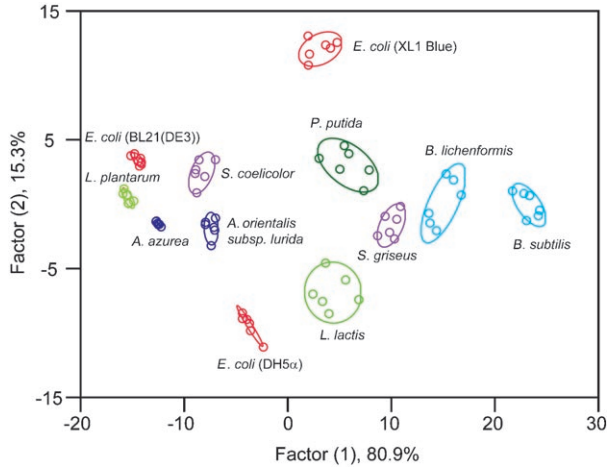


***Figure 4.*** Canonical score plot for the fluorescence response patterns as determined with LDA. The first two factors collate 96.2% of the variance. 95% confidence ellipses for the individual bacteria are depicted.

which are clustered into twelve groups according to the individual bacteria. The jackknifed matrix (with cross-validation) in LDA reveals a completely accurate classification. We can discern all twelve microorganisms, which contain both Gram-positive (e.g. *A. azurea*, *B. subtilis*) and Gram-negative (e.g. *E. coli, P. putida*) species. The LDA plot places neither the Gram-negative nor Gram-positive bacteria into a specific part of the graph, suggesting that other effects are also involved in the discrimination process. Significantly, different strains of *E. coli* can be easily discerned with the current sensor array, but the three *E. coli* strains are not grouped particularly close in the LDA plot, indicating that subtle differences in the bacteria generate marked changes in response. Although the concept introduced herein is useful, it should be noted that the present system can merely differentiate bacteria in a clean, buffered solution. Although it is suitable to analyze many biological and environmental samples, preseparation is probably required for most biological fluids as the concomitant proteins may affect the analytical results. In this regard, the introduction of recognition elements specific for a bacterial surface onto the nanoparticles would address this problem. Work in this area is currently underway.

With the patterns shown in Figure 3 and in the Supporting Information (Table S2 as the training matrix, 3 constructs × 12 bacteria × 6 replicates), we can identify unknown solutions of bacteria, randomly selected from the twelve bacterial species grown in different batches. Fluorescence response patterns generated from the three nanoparticle–polymer constructs were analyzed by LDA. After transformation of the patterns to the canonical scores using the discriminant functions established on the training samples, the Mahalanobis distances of the new case to the respective centroids of twelve groups were calculated. The closer a specific data set is to the center of one group, the more likely it belongs to that group. This assignment is based on the shortest Mahalanobis distance to the twelve bacteria in a three-dimensional space (canonical factors 1 to 3). For the 64 samples studied, 61 were correctly identified; a detection accuracy of more than 95% demonstrates expediency and reliability. The differentiation of the three strains of *E. coli* suggests suitable identification of pathogenic strains of normally harmless bacteria.

In conclusion, the integration of cationic gold nanoparticles with conjugated polymers provides an easily accessible yet potentially powerful biodiagnostic tool, in which the functional nanoparticles and the fluorescent polymer serve as the recognition elements and the transducer, respectively. The efficient quenching ability of gold nanoparticles coupled with the molecular-wire effect of conjugated polymers compound the pronounced fluorescence response, which is dictated by the binding strength of the bacterium to the gold nanoparticle. Therefore, manipulating the surface chemistry of gold nanoparticles and the constitution of the conjugated polymer will result in constructs with expanded binding capabilities. Currently, we are investigating the mechanism of binding which occurs between the hydrophobic nanoparticles and the conjugated polymer to understand the specific factors which govern fluorescence recovery. Based on our ability to readily differentiate twelve different bacteria using only three systems, we speculate that the detection of any microorganism including the differentiation of pathogenic and resistant strains will be possible with this approach.

## Experimental Section

**Sw-$CO_2$**[22] and **NP1**-**NP3**, core diameter ca. 2 nm, were synthesized according to Reference [16]. The number average molecular weight ($M_n = 14$ kDa), polydispersity index (PDI = 1.8), and degree of polymerization ($P_n = 12$) of **Sw-$CO_2$** were determined by gel permeation chromatography.[22] The bacterial stocks (see Supporting Information, were donated by Dr. A. Bommarius (Georgia Institute of Technology) and Dr. J. Hardy (University of Massachusetts at Amherst). Bacterial cells were grown in Luria broth agar medium (3 mL) at 37°C to an optical density of 1.0 at 600 nm. The cultures were centrifuged (4000 rpm, 15 min) and washed with phosphate buffer (5 mM, pH 7.4) three times, resuspended in phosphate buffer, and diluted to an absorbance of 1.0 at 600 nm.

Fluorescence titration experiments determined the complexation between nanoparticles and **Sw-$CO_2$**. Fluorescence intensity changes at 463 nm were recorded with an excitation wavelength of 400 nm; **Sw-$CO_2$** and stoichiometric amounts of **NP1**–**NP3**, as determined by the fluorescence titration study (see Table S1 in the Supporting Information), were diluted with phosphate buffer (5 mM, pH 7.4) to solutions with a final **Sw-$CO_2$** concentration of 100 nM. Each solution (200 μL) was placed into a well on the microplate. After incubation for 15 min, the fluorescence intensity at 463 nm was recorded with an excitation wavelength of 400 nm. Next, 10 μL of a bacterial solution ($OD_{600} = 1.0$) was added to each well. After incubation for another 15 min, the fluorescence intensity at 463 nm was measured again. The fluorescence intensity before addition of the bacteria was subtracted from that obtained after addition of the bacteria to record the overall fluorescence response ($\Delta I$). This process was completed for twelve

  

bacteria to generate six replicates of each, leading to a training data matrix of 3 constructs × 12 bacteria × 6 replicates (Supporting Information, Table S2) that was subjected to a classical linear discriminant analysis (LDA) using SYSTAT (version 11.0). The Mahalanobis distances of each individual pattern to the centroid of each group in a multidimensional space were calculated, and the case was assigned to the group with the shortest Mahalanobis distance. A similar procedure was also performed to identify 64 randomly selected bacterial samples based on their fluorescence response patterns. The classification of new cases was achieved by computing their shortest Mahalanobis distances to the groups generated through the training matrix. During the identification of unknown bacteria, the bacterial samples were randomly selected from the twelve respective bacteria and the solution preparation, data collection, and LDA analysis were each performed by three different researchers, resulting in a double-blind process.

Received: July 26, 2007
Revised: October 10, 2007
Published online: January 28, 2008

**Keywords:** bacteria · bioanalysis · biosensors · conjugated polymers · gold nanoparticles

[1] A. K. Deisingh, M. Thompson, *Analyst* **2002**, *127*, 567 – 581.
[2] V. Berry, A. Gole, S. Kundu, C. J. Murphy, R. F. Saraf, *J. Am. Chem. Soc.* **2005**, *127*, 17600 – 17601.
[3] M.-C. Daniel, D. Astruc, *Chem. Rev.* **2004**, *104*, 293 – 346.
[4] a) S. W. Thomas, G. D. Joly, T. M. Swager, *Chem. Rev.* **2007**, *107*, 1339 – 1386; b) I. B. Kim, J. N. Wilson, U. H. F. Bunz, *Chem. Commun.* **2005**, 1273 – 1274.
[5] N. L. Rosi, C. A. Mirkin, *Chem. Rev.* **2005**, *105*, 1547 – 1562.
[6] X. Zhao, L. R. Hilliard, S. J. Mechery, Y. Wang, R. P. Bagwe, S. Jin, W. Tan, *Proc. Natl. Acad. Sci. USA* **2004**, *101*, 15027 – 15032.
[7] C. R. Bertozzi, M. D. Bednarski, *J. Am. Chem. Soc.* **1992**, *114*, 2242 – 2245.
[8] R. I. Amann, W. Ludwig, K.-H. Schleifer, *Microbiol. Rev.* **1995**, *59*, 143 – 169.
[9] B. S. Reisner, G. L. Woods, *J. Clin. Microbiol.* **1999**, *37*, 2024 – 2026.
[10] See Table S5 and extra citations in the Supporting Information.
[11] M. B. Edmond, S. E. Wallace, D. K. McClish, M. A. Pfaller, R. N. Jones, R. P. Wenzel, *Clin. Infect. Dis.* **1999**, *29*, 239 – 244.
[12] C. A. Batt, *Science* **2007**, *316*, 1579 – 1580.
[13] P. D. Frenzen, A. Drake, F. J. Angulo, *J. Food Prot.* **2005**, *68*, 2623 – 2630.
[14] P. S. Mead, L. Slutsker, V. Dietz, L. F. McCaig, J. S. Bresee, C. Shapiro, P. M. Griffin, R. V. Tauxe, *Emerging Infect. Dis.* **1999**, *5*, 607 – 625.
[15] C. Fan, K. W. Plaxco, A. J. Heeger, *J. Am. Chem. Soc.* **2002**, *124*, 5642 – 5643.
[16] C.-C. You, O. R. Miranda, B. Gider, P. S. Ghosh, I.-B. Kim, B. Erdogan, S. A. Krovi, U. H. F. Bunz, V. M. Rotello, *Nat. Nanotechnol.* **2007**, *2*, 318 – 323.
[17] Dynamic light scattering (DLS) investigation revealed that the gold nanoparticles used in this study have a hydrodynamic diameter of 8–9 nm.
[18] C. M. Niemeyer, *Angew. Chem.* **2001**, *113*, 4254 – 4287; *Angew. Chem. Int. Ed.* **2001**, *40*, 4128 – 4158.
[19] I. B. Kim, B. Erdogan, J. N. Wilson, U. H. F. Bunz, *Chem. Eur. J.* **2004**, *10*, 6247 – 6254.
[20] Q. Zhou, T. M. Swager, *J. Am. Chem. Soc.* **1995**, *117*, 12593 – 12602.
[21] a) Teichoic acids and lipoteichoic acids are present on the surface of Gram-positive bacteria, whereas the outer membranes of Gram-negative bacteria are composed of lipopolysaccharides (LPSs). Furthermore, the membranes of most bacteria contain a large amount of anionic phospholipids (e.g. phosphatidylglycerol), making the bacterial surface negatively charged; b) M. Kates in *Handbook of Lipid Research: Glycolipids, Phosphoglycolipids and Sulfoglycopids* (Ed.: M. Kates), Plenum, Oxford, **1990**, pp. 123 – 234; c) B. Dmitriev, F. Toukach, S. Ehlers, *Trends Microbiol.* **2005**, 13, 569 – 574; d) A. L. Koch, *Clin. Microbiol. Rev.* **2003**, *16*, 673 – 687; e) C. Schaffer, P. Messner, *Microbiology* **2005**, *151*, 643 – 651; f) M. P. Bos, B. Tefsen, J. Geurtsen, J. Tommassen, *Proc. Natl. Acad. Sci. USA* **2004**, *101*, 9417 – 9422.
[22] I. B. Kim, R. Phillips, U. H. F. Bunz, *Macromolecules* **2007**, *40*, 5290 – 5293.
[23] R. G. Brereton in *Chemometrics: Data Analysis for the Laboratory and Chemical Plant*, Wiley, New York, **2003**.
[24] P. C. Jurs, G. A. Bakken, H. E. McClelland, *Chem. Rev.* **2000**, *100*, 2649 – 2678.

  